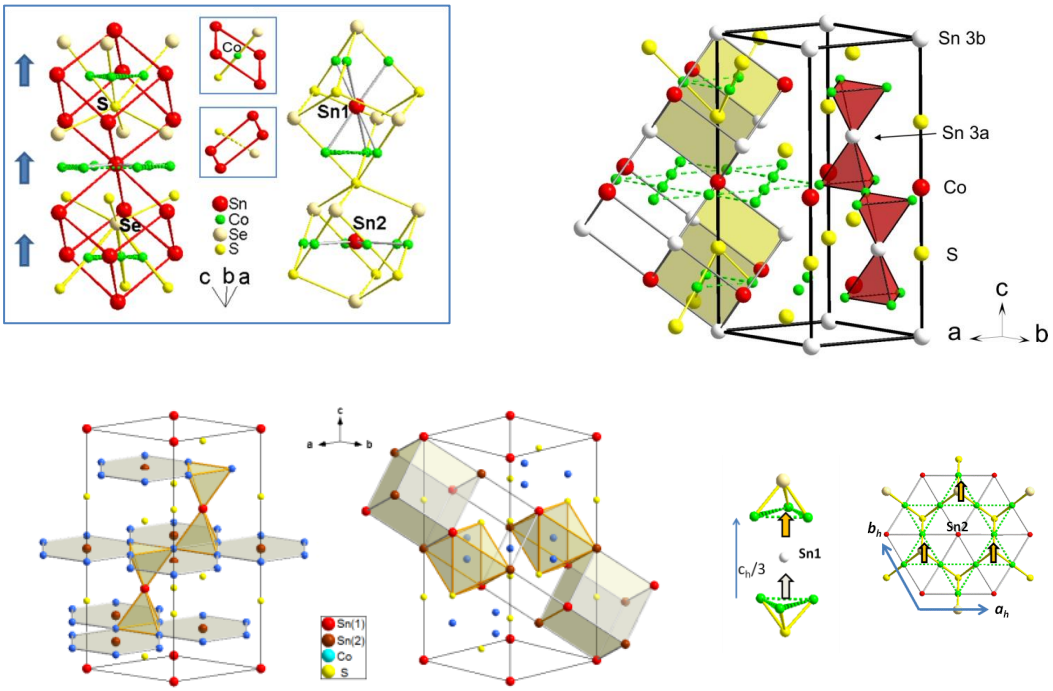

Fig. S1: Alternative representations of the shandite structure

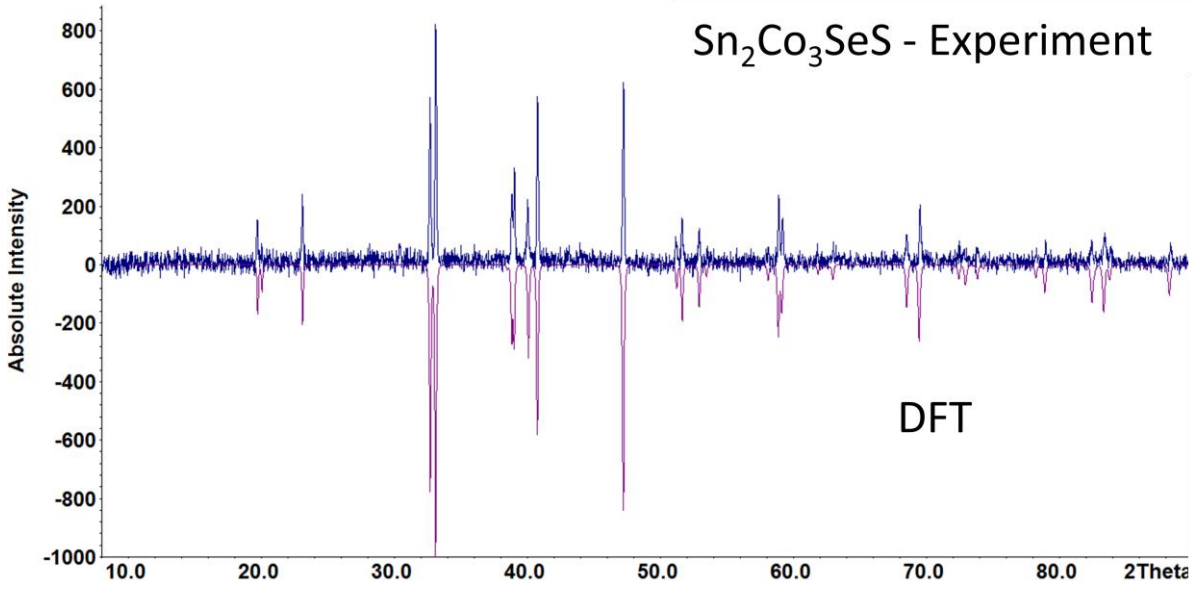

Fig. S2: Comparison of experimentally obtained X-ray diffraction pattern and simulated diffractrogram from DFT predictions.

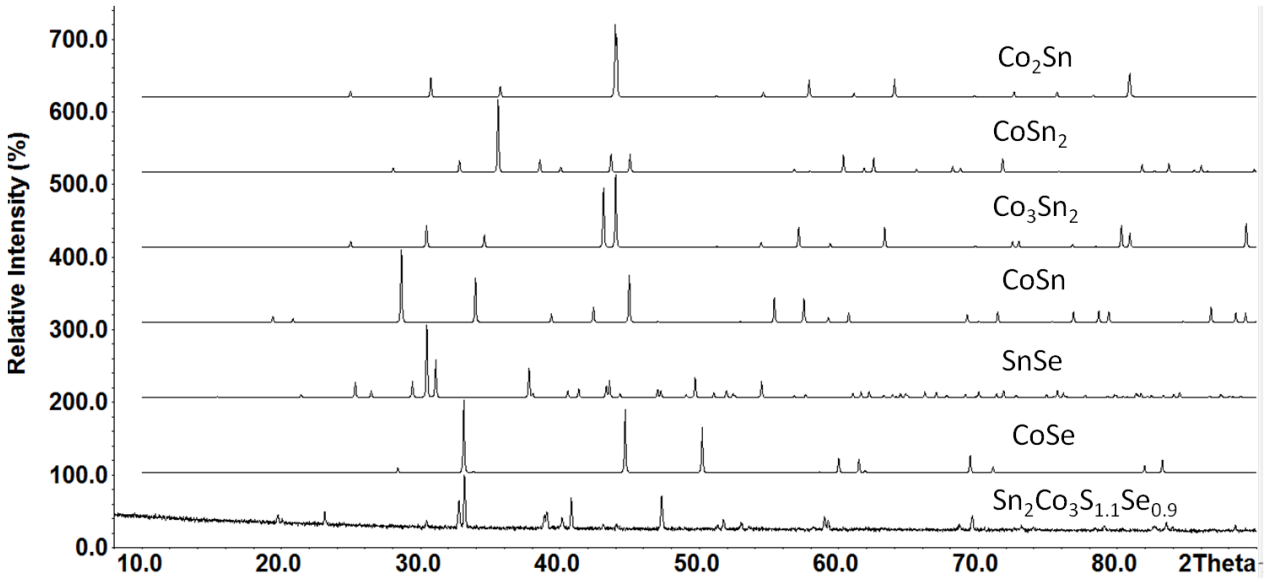

Fig. S4: Analysis of impurities for the x = 1.9 sample.

a)

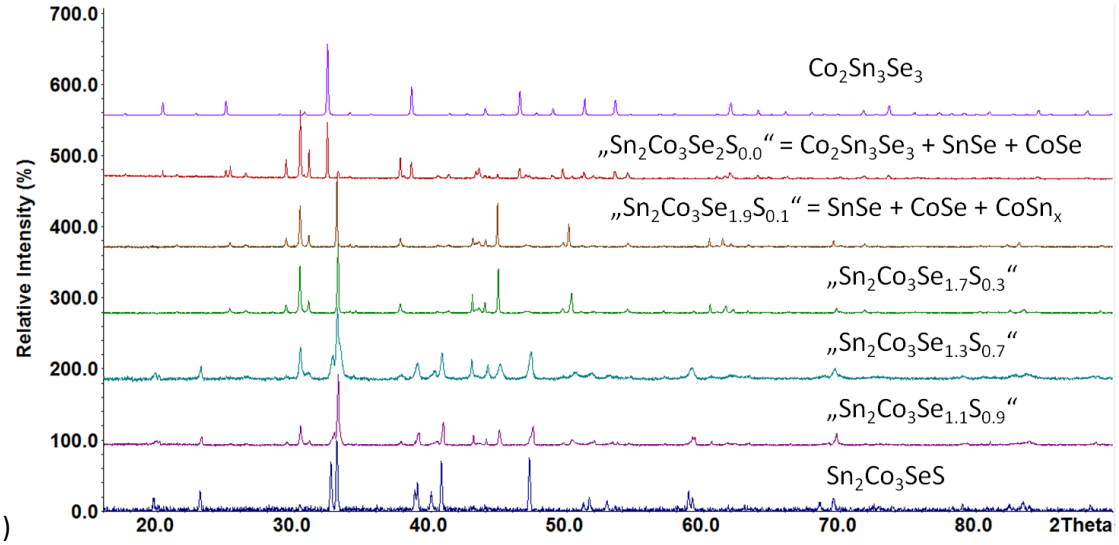

b)

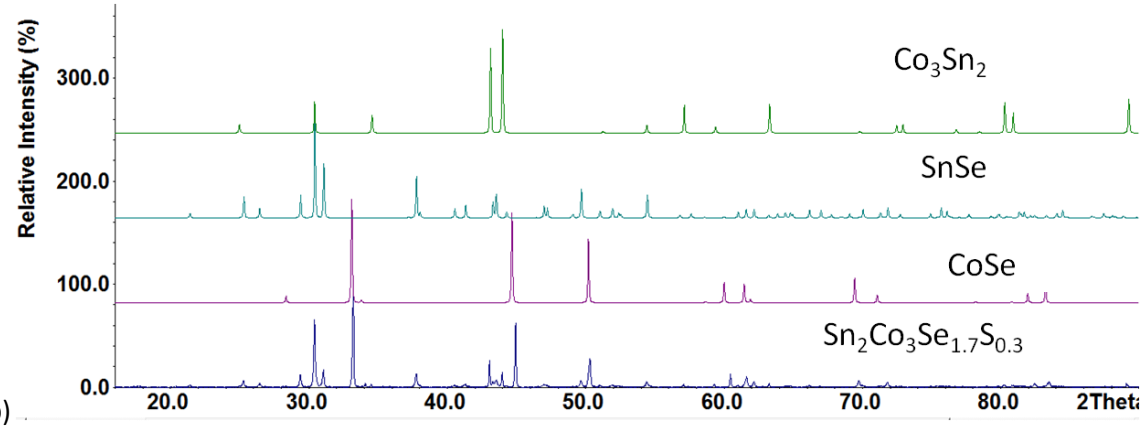

Fig. S5 a) Diffraction patterns for x(Se) = 1.0, 1.1, 1.3, 1.7, 1.9, and 2.0 with comparison to skutterudite type $Co_2Sn_3Se_3$, b) analysis of the phases in the sample for x = 1.7 with CoSe, SnSe, and Co_3Sn_2. Mind that substitution of Se by S (1.7 : 0.3) causes tiny shifts of reflections.

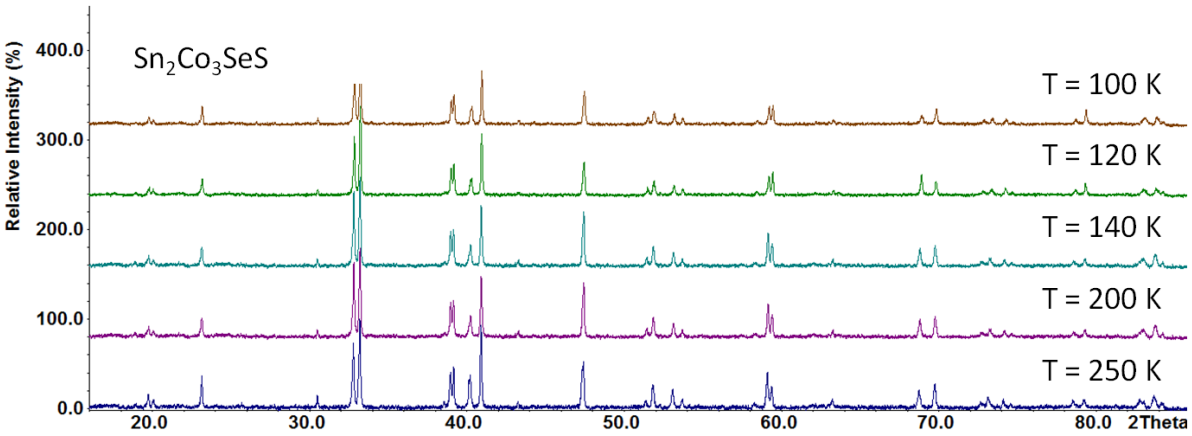

Fig. S5c: Temperature dependent X-ray diffraction patterns for Sn_2Co_3SeS.

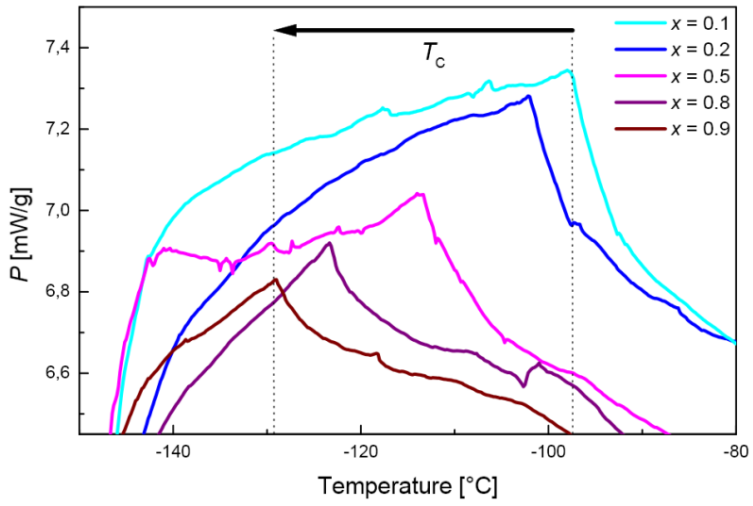

Fig. S6: DSC measurements on $Sn_2Co_3S_{2-x}Se_x$ (heating curves)

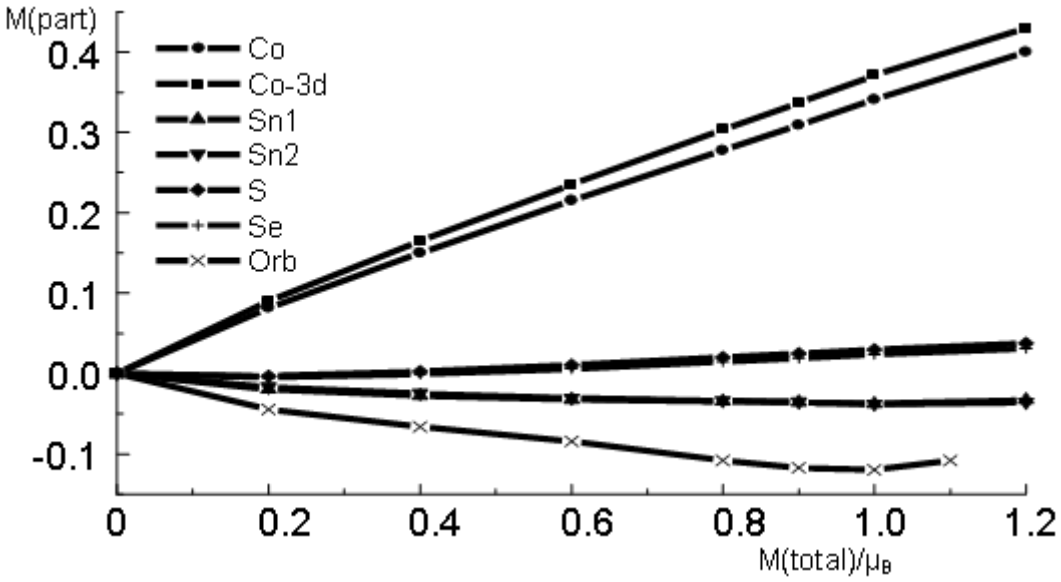

Fig. S7: Atomic projected spin polarisation and orbital magnetisation

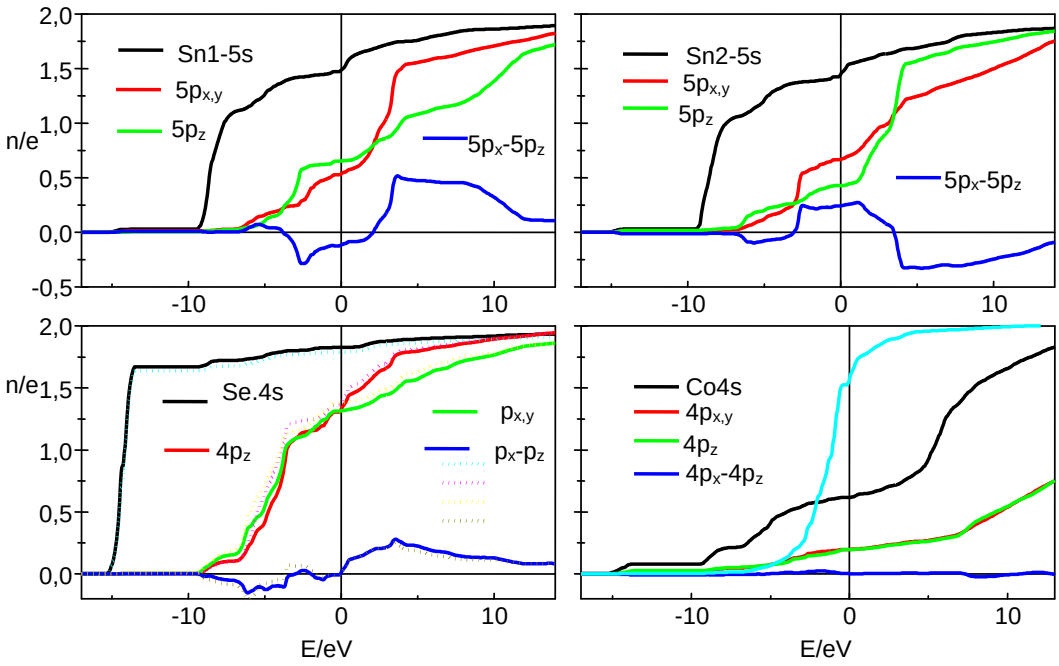

Fig. S8: Atomic orbital projected integrated DOS

Tab. S1: Calculated atomic charges in $Sn_2Co_3S_{1-x}Se_x$ (FPLO)

x(Se)	N(e) Sn1	Q	N(e) Sn2	Q	N(e) Co	Q Co	N(e) S	Q S	N(e) Se	Q Se
0	49.32	+0.68	49.32	+0.68	27.19	-0.19	16.40	-0.40		
1	49.40	+0.60	49.40	+0.60	27.20	-0.20	16.42	-0.42	34.17	-0.17
2	49.48	+0.52	49.50	+0.50	27.22	-0.22			34.18	-0.18

Tab. S2: Charge density analysis for $Sn_2Co_3S_{1-x}Se_x$

x(Se)	ρ°-Sn1 e/au	ρ°-Sn2 e/au	EFG - VZZ1	EFG - VZZ2
0	86625.05	86625.10	-2.42	3.22
1	86625.05	86625.17	-2.32	3.14
2	86625.10	86625.27	-2.23	3.21